SYNERGY BETWEEN EROSION-CORROSION OF STEEL AISI 4140 COVERED BY A MULTILAYER TiCN / TiNbCN, AT AN IMPACT ANGLE OF 90°

SINERGIA ENTRE LA CORROSIÓN EROSIÓN DEL ACERO 4140 RECUBIERTO POR MULTICAPAS DE TiCN / TiNbCN, A UN ÁNGULO DE IMPACTO DE 90°

WILLIAN APERADOR CHAPARRO
Ph.D. Profesor, Facultad de Ingeniería, Universidad Militar Nueva Granada, Colombia, g.ing.materiales@gmail.com

CARLOS RAMÍREZ MARTIN
MSc. Departamento de Física, Universidad de Boyacá, Tunja, Boyacá-Colombia, carama71@gmail.com

ENRIQUE VERA LÓPEZ
Ph.D. Profesor, Universidad Pedagógica y Tecnológica de Colombia, corrosion_total@yahoo.es

ABSTRACT: The aim of this work is the study of the effect of corrosion erosion on wear for [TiCN / TiNbCN] n multilayer coatings on AISI 4140 steel substrates. We have grown [TiCN/TiNbCN] n multilayered via reactive RF (radio frequency) magnetron sputtering technique in which systematically the bilayer period (Λ) and the bilayer number (n were varied), maintaining the total thickness of the coatings constant ($\sim$ 3 μm). The multilayers were evaluated and compared for corrosion, erosion and erosion-corrosion at an impact angle of 90º in a solution of 0.5 M NaCl and silica which simulates a marine environment, analyzing the effect of the number of bilayers on the corrosion resistance of these coatings. Polarization curves were conducted at rest potential. After the polarization experiments the specimens were analysed by scanning electron microscopy. The results show good performance of the multilayer systems in dynamic corrosion systems and erosion-corrosion, furthermore the enhancement of wear is due to the fact that the polarizations curves move towards areas where current densities decrease by increasing the bilayer number.

KEYWORDS: Wear, multilayer system, synergy, impact angle of 90º.

RESUMEN: El propósito de este trabajo es estudiar el efecto de la erosión corrosión en el desgaste de los recubrimientos en forma de multicapas de [TiCN / TiNbCN] n depositadas sobre sustratos de acero AISI 4140. El crecimiento de las multicapas de [TiCN / TiNbCN] n se realizó mediante un sistema magnetrón sputtering con RF reactivo en el que se varió sistemáticamente el período bicapa (Λ), y el número bicapa (n), manteniendo constante el espesor total de las capas ($\sim$ 3 micras). Las multicapas se evaluaron comparando la corrosión, erosión y erosión – corrosión a un ángulo de impacto de 90 ° en una solución de 0,5 M de NaCl y de sílice, analizando el número de bicapas sobre en la resistencia a la corrosión de estos recubrimientos. Las curvas de polarización se realizaron en el potencial de reposo. Posteriormente de la realización de los experimentos de las curvas de polarización las muestras se analizaron por microscopía electrónica de barrido. Los resultados muestran que el buen rendimiento de los sistemas multicapa en sistemas dinámicos de corrosión y corrosión por erosión y la mejora de desgaste es debido al hecho de que las curvas de polarización se mueven hacia las zonas donde las densidades de corriente disminuyen al aumentar el número de bicapas.

PALABRAS CLAVE: Desgaste, sistema multicapa, sinergia, ángulo de impacto de 90°

1. INTRODUCTION

Erosion-corrosion is an accelerated corrosion of metals due to a combination of chemical attack and abrasion by physical movement of fluids with suspended solids. Alloys that form film surfaces in a corrosive environment commonly have a corrosion speed limit above which corrosion is accelerated rapidly. Erosion-corrosion is associated with current induced by mechanical removal surface of the protective film that results in a further increase of corrosion rates for chemical or electrochemical processes. Surface engineering of metallic substrates with protective film calls for a lot of attention from industry and researchers,

as it produces a host of properties such as wear and erosion resistance, and oxidation and corrosion resistance. However, a coating is highly functional only if the interface between the film and the substrate is sound and strong. [1-3] In recent years, much research has been aimed at developing multilayered structures of nanometric period thickness, also called superlattices, for their use as protective hard coatings. The advantage of such structures rests on their improved mechanical and tribological properties, compared with those of their individual components [4–9].

Hardness enhancements in thin film isostructural superlattices have been successfully modeled by dislocation image force theories, arising from Koehler's first model [10] based on shear modulus differences, in combination with Chu and Barnett's correction assuming dislocation propagation inside monolayers [11]. Moreover, there have also been reports of mechanical and electrochemical enhancements in isostructural superlattices [12-14]. Among these isostructural systems, metal/ceramic and ceramic/ceramic superlattices have been receiving major attention since this combination can exhibit high hardness values, while retaining good ductility and high anticorrosive properties. Several of these superlattices have been studied during the past 10 years including Ti/TiN [12], TiN/V0.3Nb0.7N [13] and TiN/NbN [14].

The nitride coatings, which are characterized by high hardness, wear resistance, and corrosion resistance, are gaining wider use for strengthening and protection of constructional steels from wear and corrosion. A significant disadvantage of such coatings limiting their use is their lack of thickness, which in many cases does not exceed 5 μm. In connection with this, the wider use of Physical Vapor Deposition (PVD) magnetron sputtering technology in the strengthening of machine parts is possible enabling the development of multilayer coatings having a higher combination of properties. One of the most important parameters determining the service properties of nitride coatings is the size and quantity of the pores, which as the result of the thinness of the protective layer go all the way through to the base and are sites of corrosion. It is known that PVD coatings have significantly less porosity in comparison with coatings obtained by other methods using vacuum technology or gas thermal spraying. In some cases magnetron sputtering makes it possible to

obtain porosity-free coatings mainly in multilayers with a thickness of the order of 1 μm, which is the result of the high packing density of the atoms being deposited. According to the data of previous works, the porosity of nitride coatings may reach 5% which differs from the multilayer nitrides where the porosity decreases to 1% [14]. Therefore the corrosion resistance of multilayer nitride coatings is higher than that of single-layer ones, which may be explained by their greater thickness and features of their microstructure, including the absence of circular crystals characteristic of single layer coatings, moreover failure of nitride coatings under the action of a corrosive medium occurs at structural defects, which determine their corrosion resistance and electrochemical properties [10].

The aim of this work is to study the effect of impact angle and the number of bilayers on the corrosion–erosion resistance of commercial AISI 4140 uncoated steel, and AISI D3 steel coated with a TiCN / TiNbCN multilayer system (with 3 μm of thickness) under corrosive slurry containing chloride ions (Cl-) and hard erosive particles

2. EXPERIMENTAL DETAILS

[TiCN/TiNbCN]$_n$ multilayers were deposited on AISI 4140 steel substrates by using a multitarget magnetron reactive sputtering technique, with an RF source (13.56 MHz) and two stoichiometric TiC and Nb targets with purities of 99.9% for both targets. The deposition parameters for obtaining high-quality coatings were a sputtering power of 400 W for TiC and 350 W for the Nb target; a substrate temperature of 300 ºC; and circular substrate rotation at 60 RPM, to facilitate the formation of the stoichiometric quaternary film. The sputtering gas was a mixture of Ar 76% (50 sccm) and N$_2$ 24% (16 sccm) with a total working pressure of 6×10^{-3} mbar. An unbalanced RF bias voltage of -50V was applied. Moreover our magnetron sputtering device has a substrate positioning system in relationship to the target spot, this parameter permits varying the bilayer number between 1, 50, 100, 150 and 200; changing the bilayer period. The measured total thickness of the deposited [TiCN/TiNbCN]n multilayers was found to be approximately 3 μm for all the samples. The individual thickness varied as a function of bilayer number from n = 1 to n = 200 producing layers with thicknesses from 1.5 μm to 7.5 nm, respectively.

For the analysis of the erosive–corrosive effect a device built for the evaluation of chemical attack in metallic materials and coated materials was used. Fig. 1 shows the erosive–corrosive test device that consists of a glass container for erosive–corrosive storage, an impeller of High Ultra Molecular Weight Polyethylene (HUMWPE) which rests on a Teflon shaft that is attached to the main motor shaft which provides fluid motion. The lid of the container allows location of the sample under an impact angle of 90º for corrosive fluid action, as well as the reference electrode and counter electrode. On the other hand, the fluid movement is caused by the motor shaft. The tangential speed applied to the fluid with erosive particles was fixed at 13 m/s, this takes into account that the impeller radius is 0.055m and the motor speed was fixed at 2250 RPM. The electrochemical study was carried out with a Gamry PCI 4 300™ Potentiostat, which has a Gamry Framework Version 4.21/DC corrosion software, the Tafel polarization curve technique was realized at room temperature using a cell that support one working electrode ([TiCN/TiNbCN]n) within an exposed area (1 cm^2), a reference electrode (Ag/AgCl) and a graphite counter electrode under a 0.5M NaCl solution in distilled water. The resting potential was measured during 30 minutes. Measurements were carried out on a set of three different identical samples. Tafel polarization curves were obtained at a sweep speed of 0.16 mV/s within a voltage range of -0.3 V to 0.3 V with an exposed area of 1 cm^2. In this work, silica (SiO$_2$) was used as an abrasive agent with a particle size between 210 μm and 300 μm. This chemical solution was chosen since it has been shown that it can be used to study steel as it facilitates the chemical attack at defined anodic region by the chloride. The molar mass of the work electrode (wE) for all tests was assumed to be 55.847g/mol taking into account the Fe (pure) as reference since this material (Fe) has a low carbon content.

The samples were subjected to wear due to erosion during 24 hours and a temperature of 25 °C. For the purpose of determining the weight loss due to erosion, during an immersion test in a solution of NaCl 0.5 M in the presence of particles of silica (SiO$_2$), samples were removed from the solution in intervals of 15 minutes, cleaned with water, dried with hot air, and weighed on a balance with a precision of 0.1 mg. The erosive phenomenon was evaluated using cathodic protection of 1V cathodic with respect to open circuit potential of both the steel and the coating respectively, according to the ASTM norm G 119-93 [20]; this cathodic protection ensures that surface damage is only caused by erosive particles.

Finally, the process of surface corrosion was analyzed and the superficial morphology was characterized by using a High-Resolution Scanning Electron Microscope (SEM) (Philips XL 30 FEG).
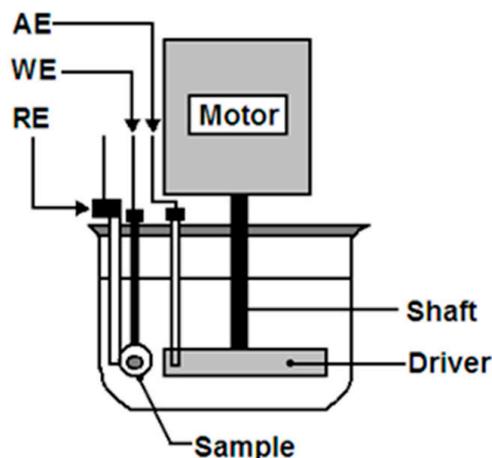
Figure 1. Schematic for device used at corrosion-erosion wear testing. In the figure, the acronyms AE, WE and RE are the auxiliary electrode, working electrode, reference electrode, respectively [1-3].

3. RESULTS AND DISCUSSION

3.1. Dynamic corrosion

According to the anodic polarization curves (corrosion potential as a function of the corrosion current density) shown in Figure 2, it can be noted that the corrosion potential in the multilayers of [TiCN/TiNbCN]n are shifted towards anodic areas (protection), therefore the influence of increasing the multilayers in raising the corrosion potential can be established, determined by a relationship represented by a linear regression (Table 1). The curves in Figure 2 show the generation of an active corrosion zone in the anode area, being more prominent for the substrate. The multilayer generates areas of lower electro-dissolution in a range of -500 mV to -110 mV relative to the start of the electro-dissolution (250mV vs. corrosion potential (Ecorr), subsequently increasing the area of active corrosion of the multilayers due to increased density of corrosion.

The steel (substrate) in a NaCl 0.5 M medium has a change in behavior in the anodic branch of a potential near to -400 mV vs. Ag/AgCl; this change can be interpreted as the start of the formation of a stable general corrosion due to a greater increase in the density of corrosion, indicating the regeneration of a layer of corrosion products that can stabilize the current density around this potential, and prevent the increase of the dissolution rate of the metal. The anodic areas generate dissolution of the coating, due to the diffusion that occurs in them. Once the passivity is destroyed, there is an increase of corrosion due to pitting, which will augment the corrosion; this feature can be seen in the entire set of potentiodynamic curves.
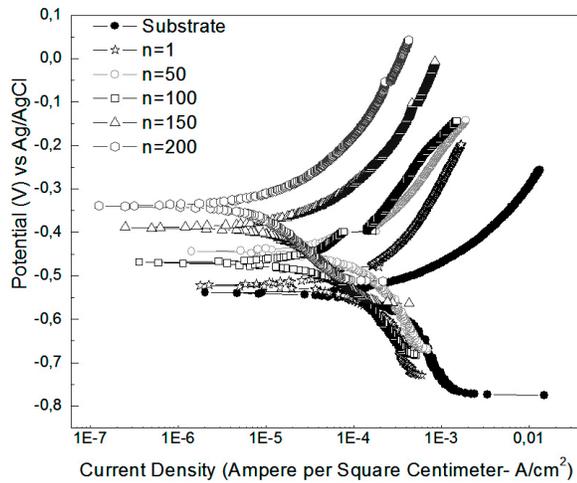
Figure 2. Polarization curves of the dynamic corrosion in a solution of 0.5 M NaCl

Table 1 shows the decrease of corrosion rate with the current density in multilayer coatings of [TiCN / TiNbCN]n; this decrease can be attributed to the degree of porosity present in the thin films, indicating that it decreases with the increase of the number of multilayers. The porosities in the multilayers may occur in the coating due to nucleation phenomena during the growth of the layers, generating paths of least resistance for the passage of the Cl ion [16]. The displacement of the Tafel curves toward positive potentials with increasing number of applied coats lies in the nature of such multilayer structures, since increasing the number of multilayers increases the number of interfaces between TiCN and TiNbCN monolayers. As the interfaces are areas which present structural disorders which generate a change in crystallographic orientation,

they act as points of dispersion, making the migration of the Cl⁻ from the surface into the metallic substrate difficult and delaying the onset of the corrosion process [4]. This explains the fact that the power required by the ions from the solution to migrate freely from the surface towards the interface film/substrate, is greater with increasing number of multilayers; this behavior reflects in the reduction of the corrosion current density and orrosion rates in micrometers per year (Table 1) [6] [21].

Table 1. Parameter values obtained by electrochemical polarization curves for the substrate and the multilayer [TiCN / TiNbCN] n.

Material	Corrosion Potential - Ecorr (mV)	Current Density Icorr ($\mu A/cm^2$)	Corrosion rate $Vcorr \times 10^{-3}$ ($\mu m\, y$)
Substrate	-538	309,1	436,96
n=1	-520	94,21	132,78
n=50	-441	64,54	90,38
n=100	-468	41,13	58,59
n=150	-389	18,41	25,39
n=200	-339	9,31	12,94

3.2. Erosion

Figure 3 graphically represents the loss of material associated with repeated impacts of solid particles after 24 hours of testing. It shows greater loss of mass over time in the substrate owing to its low ductility multilayer coatings of [TiCN / TiNbCN]n generating a decrease in mass loss; the sample with multilayers reduced mass loss by 53% regarding the uncoated substrate, showing the beneficial effect of the implementation of the AISI 4140 steel films. The sample coated with 200 multi-layers had the lowest value of mass loss; this behavior can be attributed to the application of more multilayers, generating improvements in the mechanical properties, especially hardness. The multilayers absorb and distribute impact energy generated by the abrasive particles in a better way. Also the mechanical properties such as hardness and elastic modulus are improved [13] [14] [15] [22].
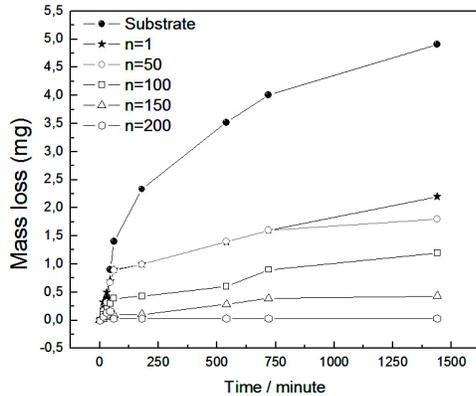
Figure 3. Mass loss as a function of the number of multilayers of [TiCN / TiNbCN] n without a corrosive effect.

3.3. Corrosion-erosion.

Figure 4 compares the performance of different multilayers [TiCN/TiNbCN]n in the erosion/corrosion system for the materials studied, in which it can be observed that the corrosion rate and corrosion current density, decreases in function of the number of multilayers. Furthermore, a generalized corrosion phenomenon can be observed in all multilayers; however the difference of values of corrosion rate is because the corrosion rate is inversely proportional to the number of bilayers, due to the kinetics of the reaction

Qualitatively it is possible to group the Tafel polarization curves, the curves of coated steel with multilayers of 150 and 200 are similar. The multilayers of [TiCN / TiNbCN] n show a moderately dissolution of the material
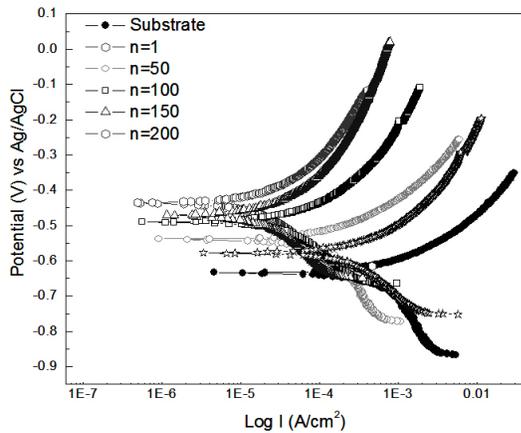
Figure 4. Polarization curves of corrosion-erosion of the substrate and the multilayer [TiCN / TiNbCN] n in 0.5M NaCl solution.

The data reported in Table 2 shows lower electrochemical performance in comparison to the dynamic corrosion (Figure 4 and Table 1) and with erosion/corrosion, which shows a decrease in corrosion potential and densities, relatively acceptable for multilayers with one multilayer or even slightly better than the multilayers 50 and 100, as well as good conditions for the multilayers 150 and 200. In general, the data in Table 1 shows a good performance of all the coatings tested –in comparison to the base material– when subjected to corrosive phenomena. However, when subjected to the corrosive-erosive flow (Table 2) the passive film formed on the surface is generally eliminated and removed by the action of hard particles, leading to loss of corrosion protection.

Table 2. Electrochemical parameters obtained from polarization curves in corrosion-erosion system for the substrate and the multilayer [TiCN / TiNbCN] n.

Material	Ecorr (mV)	Icorr ($\mu A/cm^2$)	Vcorr$\times 10^{-3}$ ($\mu m y$)
Substrate	-633	706	995,46
n=1	-579	374	527,34
n=50	-538	186	262,26
n=100	-490	51	71,91
n=150	-469	26	33,26
n=200	-438	17	21,65

The calculations of synergy allow to establish how the essential conditions of wear (mechanical and electrochemical) interact with each other, either to mitigate or enhance one of two mechanisms or to contribute to the overall process of wear of materials. Hence the importance of quantifying its value through the equations described below.

Equation 1. Total weight loss by erosion corrosion

$$TWL = E + C + S \tag{1}$$

Equation 2. Total weight loss account for additive effects and synergistic

$$TWL = E + C_0 + \Delta C_E + \Delta E_C \tag{2}$$

where:

$$\Delta E_C = S \quad \wedge \quad C = C_0 + \Delta C_E \tag{3}$$

$$C = \frac{i \times W \times A \times T}{F \times n} \tag{4}$$

Parameters of the equations (mg):

TWL: Total loss by erosion corrosion

E: Loss by erosion

C: Electrochemical corrosion loss between erosive

C_0:   Electrochemical corrosion loss in dynamic environment

ΔC_E: Additive effect on the corrosion erosion

S: Synergistic effect on the erosion corrosion

i: i_{corr} Corrosion current density ($\mu A/cm^2$)

W: atomic weight (g/mol)

A: exposed area (cm^2)

T: Exposure time (s)

F: Faraday constant (96500 C)

n: Number of ions

Figure 5 and Table 2 show the combined effect of wear and corrosion, which generates a much larger loss of material than the additive effect of each process; taken independently it leads to a synergism between these two processes. It is noted that corrosion can occur in the absence of mechanical wear, and that in erosion wear, no corrosion phenomena was produced because of the applied cathodic protection.

When observing the magnitude of the synergism for each of the materials studied, it is observed that the performance of the wear mechanisms is implicitly related to the aggressiveness or environmental effect on the material, because in the electrolyte of NaCl there are positive values of this parameter observed (Table 3). Performing a detailed analysis of the performance of mechanisms in the marine environment, it is observed that the material with the highest synergistic effect is for carbon steel, while the multilayers show decreasing values according to the number of the multilayers. This effect is primarily due to the action of the chloride ion, since the depolarization generated in the system, promotes localized corrosion phenomena which

advance towards the substrate without expanding the affected areas, the ridges generated by the pitting, decrease the amount of electrolyte contained therein. This result indicates that the micro mechanisms of wear are responsible for the presence and progress of localized corrosion phenomena and favor a greater removal of the outer layers of the multilayers.
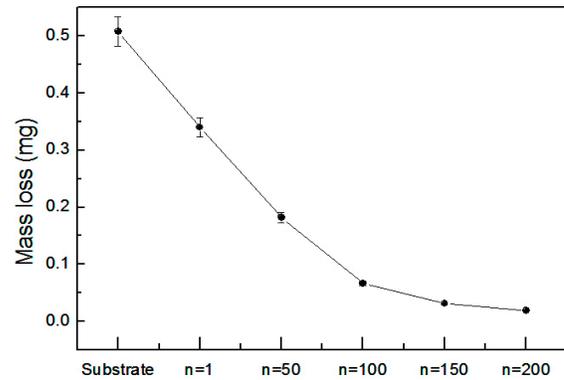
Figure 5. Mass loss with corrosive effect as function of bilayer number for impact angles 90°.

Table 3. Calculation of wear corrosion interaction for the substrate and the multilayer [TiCN / TiNbCN] n.

Material	TWL	C	E	S
Substrate	1.54	0.037	0.50	0.995
n=1	0.82	0.011	0.33	0.476
n=50	0.40	0.0078	0.18	0.216
n=100	0.11	0.0050	0.06	0.040
n=150	0.052	0.0021	0.06	0.018
n=200	0.033	0.0011	0.019	0.013

3.4. Scanning electron microscopy.

The micrographs in Figure 6 show the results of corrosive attack. These micrographs are taken at the surface of the substrate and the multilayer with 1, 100 and 200 multilayers after the erosion/corrosion process at an impact angle of 90°. In Figure 6a an area of the substrate can be seen which has been deteriorated due to the effect of dynamic corrosion. In Figure 6c the way in which the coating has undergone wear mechanisms by cracking can be seen; different zones can be distinguished, demonstrating: 1) the degradation due to general corrosion shown in the polarization curves and 2) adverse effect generated by the action

of corrosion and cracking of the coating produced by the impact energy of the abrasive particles of silica. There are also gray areas where the protective effect has generated defense mechanisms, producing zones of low cracking; these areas show a surface without fractures protected by the multilayers. It can be observed on the surface of the 200 multilayer coating, foci of localized corrosion, which can be associated with the response generated in the anodic polarization curves, wherein at -135 mV vs. Ag/AgCl, pitting attack occurs.

(a)   (b)

(c)   (d)

(e)   (f)
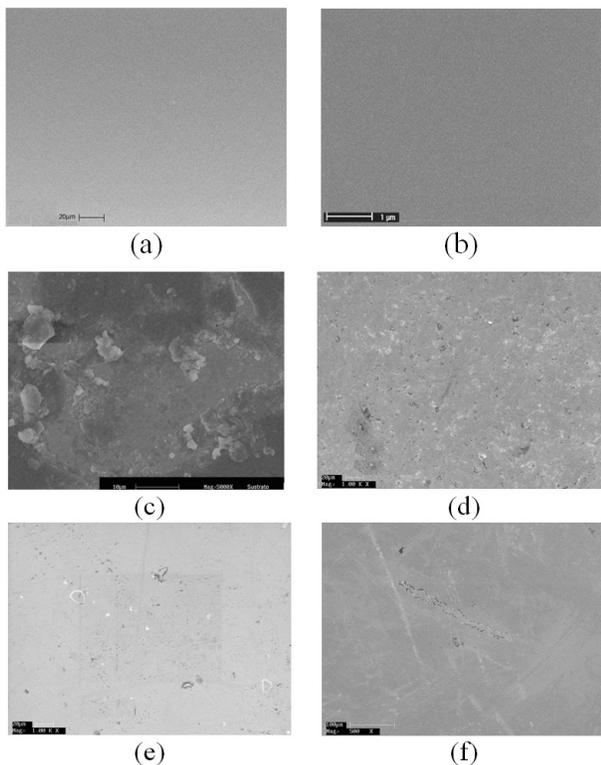
Figure 6. SEM micrographs for samples with and without degradation (a) AISI 4140, without exposure: (b) [TiCN/TiNbCN]n with n = 200 bilayers without exposure c) Substrate with exposure to corrosion erosion; d) multilayer [TiCN / TiNbCN] n with n = 1 with exposure to corrosion erosion, e) multilayer [TiCN / TiNbCN] n with n = 100 with exposure to corrosion erosion, f) multilayer [TiCN / TiNbCN] n with n = 200 with exposure to corrosion erosion.

4. CONCLUSIONS

In general it can be concluded that the dominant mechanism of wear is erosion, followed by erosion / corrosion and then corrosion. It was also observed that the corrosion benefits from the dynamic changes

of the environment and furthermore, from the action of the impact on the surface, whether or not it leads to its hardening, because the result of removing the outer layers of material or, alternatively, deforming them, increases the surface area exposed and the ability to react to the surrounding environment. Agitation also promotes the decrease in the boundary layer of electrolyte on the surface of the material, which favors a dominant mechanism of diffusion of oxygen dissolved and ionic species into the surface of the material. We note then that according to this pattern of ideas, in the marine environment the erosive condition contributes to an increased electrochemical wear of the material. In the synergy mechanism of corrosion/erosion the simultaneity of the processes was evident: mechanical material removal (multilayer and substrate) through erosion and electrochemical corrosion process.

Tafel polarization curves obtained in the dynamic corrosion and erosion/corrosion tests show a good performance by the multilayers owing to an increased shift towards positive potentials as the number of multilayers are increased. In addition, it is observed how the behavior is improved regarding corrosion/ erosion with multilayer coatings, as evidenced by the displacement of the curves towards lower current density values with respect to the substrate; also this behavior is enhanced with the increase of the period of the multilayers. All Tafel polarization curves indicate an overall dissolution and subsequent localized corrosion; this behavior is due to the aggressive effect generated by the joint corrosion and erosion. It is suggested that the coatings are treated with a cathodic protection system so that the pitting corrosion rate does not affect the coating in aggressive conditions.

ACKNOWLEDGEMENTS

REFERENCES

[1] Aperador, W., Caicedo, J.C., España, C., Cabrera, G. and Amaya, C., Bilayer period effect on corrosion–erosion resistance for [TiN/AlTiN]n multilayered growth on AISI 1045 steel. Journal of Physics and Chemistry of Solids, 71(12), pp. 1754-1759, 2010.

[2] Caicedo, J. C., Cabrera, G., Aperador, W., Escobar, C. and Amaya, C., Corrosion-Erosion Effect on TiN/TiAlN Multilayers. Journal of materials engineering and performance. 21(9), pp. 1949-1955, 2012.

[3] Aperador, W., Ramírez, C. and Bautista, J., Sinergia entre la corrosión erosión del acero 1045 recubierto por multicapas de TiN/TiAlN. Revista Mexicana de Física. 57(4), pp. 350–355, 2011.

[4] Aperador, W., Amaya, C. and España, C., Resistencia a la corrosión de las multicapas de [TiN/AlTiN]n Depositadas sobre acero al carbono AISI 1045. Revista Dyna, 78(165), pp. 183- 189, 2011.

[5] Holmberg, K., Matthews, A. and Ronkainen, H., Coatings Tribology- contact mechanisms and surface design. Tribol. Int., 31(1-3), pp. 107–120, 1998.

[6] Nieto, J., Caicedo, J., Amaya, C., Moreno, H., Aperador, W., Tirado, L. and Bejarano, G., Evaluación de la influencia del voltaje bias sobre la resistencia a la corrosión de películas delgadas de AlNbN. Dyna, 77(162), pp. 161-168, 2010.

[7] Junhua, X., Geyang, Li. and Mingyuan, Gu., The microstructure and mechanical properties of TaN/TiN and TaWN/TiN superlattice films. Thin Solid Films, 370(1–2), pp 45-49, 2000.

[8] Philip, Y. C. and Sproul, W.C., Nanometer scale multilayered hard coatings. Vacuum, 55(3), pp. 179-190, 1999.

[9] Caicedo, J.C., Amaya, C., Yate, L., Aperador, W., Zambrano, G., Gómez, M.E., Alvarado-Rivera, J., Muñoz-Saldaña, J. and Prieto, P., Effect of applied bias voltage on corrosion-resistance for $TiC_{1-x}N_x$ and $Ti_{1-x}Nb_xC_{1-y}N_y$ coatings. Applied Surface Science, 256(9), pp. 2876-2883, 2010.

[10] Koehler. J. S., Attempt to Design a Strong Solid. Phys. Rev. B. 2(2), pp. 547–551, 1970.

[11] Chu, X. and Barnett, S.A., Model of superlattice yield stress and hardness enhancements. Journal of Applied Physics, 77(9), pp. 4403–4412, 1995.

[12] Barshilia, H. C., Deepthi, B., Selvakumar, N., Jain, Anjana. and Rajam, K.S., Nanolayered multilayer coatings of CrN/CrAlN prepared by reactive DC magnetron sputtering. Applied Surface Science, 253(11), pp. 5076-5083, 2007.

[13] Barshilia, H. C., Deepthi, B., Rajam, K. S., Bhatti,

Kanwal P-reet; Chaudhary, S., Growth and characterization of TiAlN/CrAlN superlattices prepared by reactive direct current magnetron sputtering. Journal of Vacuum Science & Technology A: Vacuum, Surfaces, and Films, 27(1), pp. 29-36, 2009.

[14] Jehn, H.A., Improvement of the corrosion resistance of PVD hard coating–substrate systems. Surface and Coatings Technology, 125(1–3), pp. 212-217, 2000.

[15] Bautista, J., Aperador, W. and España, C., Desgaste abrasivo y corrosivo de recubrimientos TiN/TiAlN y TiN/AlTiN, Alemania, Editorial Académica Española, pp. 45-65, 2011.

[16] Caicedo, J. C., Amaya, C., Yate, L., Aperador, W., Gómez, M. E. and Prieto, P., Improvement of the electrochemical behavior of AISI 4140 steel substrate using [TiCN/TiNBCN]N multilayers system, En: In: Niobium: Properties, Production and Applications, Hauppauge NY, United States of America   Editorial Nova Science Publishers Inc, Chapter 6. pp. 123-132, 2011.

[17] Kim, J. O., Achenbach, J. D., Shinn, M. and Barnett, S. A., Elastic constants of single-crystal transition-metal nitride films measured by line-focus acoustic microscopy. Journal of Applied Physics, 72(5), pp.1805- 1815, 1992.

[18] ASTM G5 Standard Reference Test Method for Making Potentiostatic and Potentiodynamic Anodic Polarization Measurements, West Conshohocken, PA, American Society for Testing and Materials, 2003.

[19] ASTM G59-04 Standard Test Method for Conducting Potentiodynamic Polarization Resistance Measurements, West Conshohocken, PA, American Society for Testing and Materials, 2004.

[20] ASTM 119(93). Standard Guide for Determining Synergism Between Wear and Corrosion. West Conshohocken, PA. American Society for Testing and Materials, 2009.

[21] Aperador, W., Ramírez, C. and Caicedo J. C., The effect of Ti(CN)/TiNb(CN) coating on erosion–corrosion resistance. Ingeniería e Investigación, 32(2), pp. 6-11, 2012.

[22] Caicedo, J.C., Amaya, C., Yate, L., Gómez, M.E., Zambrano, G., Alvarado-Rivera, J., Muñoz-Saldaña, J. and Prieto, P., TiCN/TiNbCN multilayer coatings with enhanced mechanical properties. Applied Surface Science, 256(10), pp. 5898–5904, 2010.